Research article

Modeling of self-tilt-up motion for a two-wheeled inverted pendulum

Shouhong Miao
Engineering Training Center, Shanghai JiaoTong University, Shanghai, People's Republic of China, and

Qixin Cao
Research Institute of Robotics, Shanghai JiaoTong University, Shanghai, China

Abstract

Purpose – The purpose of this paper is to present a two-wheeled inverted pendulum with self-tilt-up motion ability. With this ability, the two-wheeled inverted pendulum can erect without assistance, and then the vehicle can be autonomously deployed. The paper proposes an approach to achieve this self-tilt-up motion, which involves precessional motion.

Design/methodology/approach – A flywheel is mounted inside the vehicle to perform high-speed spinning. The flywheel and body of the vehicle are forced to move around a fixed point and precessional motion occurs. As a result of the precessional motion, a moment is synchronously generated to tilt the body up to the upright position. Since no external force is applied on this two-wheeled inverted pendulum, it is called self-tilt-up motion. A 3D model and a prototype are built to validate this approach.

Findings – The simulation and experimental results show that the self-tilting-up motion is successful.

Research limitations/implications – This paper presents a self-tilt-up motion for a two-wheeled inverted pendulum. With the analysis of the dynamics, simulation demonstrations and prototype development, the results show that the vehicle could perform self-tilt-up motion without any assistance. The principle of this self-tilt-up motion involves processional motion of rigid body. We also pointed out the factors that play important roles in influencing the performance of self-tilt-up motion and then define the switching time for the motion to switch to dynamic balance movement.

Originality/value – Traditional multi-wheel robots cannot work when they overturn. However, the two-wheeled inverted pendulums with self-tilt-up ability do not have this shortcoming. They can stand up to keep working even if they fall down. A two-wheeled inverted pendulum with self-tilt-up ability can be applied to many places. Equipped with solar battery, it can be used as an independent explorer. This type of vehicle can be deployed in swarms for planetary detection. For example, many small two-wheeled inverted pendulums assist a lunar rover for exploration, samples gathering, etc.

Keywords Robotics, Motion, Stability (control theory)

Paper type Research paper

1. Introduction

Recently, most studies on the two-wheeled inverted pendulum focus on its balancing stability and mobility; this is due to the inherent unstable dynamics of the systems. Ha and Yuta (1996) proposed a trajectory-tracking control algorithm using a linear state-space model. In 2002, Grasser *et al.* (2002) built a two-wheeled inverted pendulum vehicle JOE. Its control system is based on two state-space controllers. Kim *et al.* (2005) applied Kane's method to analyze a 3-DOF modeling of two-wheeled inverted pendulum and to design the controller. Segway™, a human transporter (2004), adopts a PID controller to accommodate the weight change from different rider. Baloh and Parent (2003) presented a self-balancing machine called B2, which is designed for an urban transportation system. They developed a six-order dynamic model for the B2. Pathak *et al.* (2005) derived the dynamic equation of wheeled inverted pendulum in terms of physical variables and studied the system's controllability. They designed a novel position stabilization controller and use the linearized form of partial feedback to derive a two-level velocity controller. Jung and Kim (2008) presented an online learning control strategy using neural network to stabilize a two-wheeled vehicle. In this literature, the authors claimed that without knowing the dynamics of the system, uncertainties in system dynamics are compensated by neural network in an online fashion. Ren *et al.* (2008) proposed a self-tuning PID control strategy for the motion control system of a two-wheeled vehicle. The controller parameters are tuned in real time to overcome the disturbances and parameter variations.

In this study, our aim is to develop a two-wheeled inverted pendulum that can self-tilt-up without assistance when it falls to the ground and then to apply it to autonomous or auxiliary field exploration where it is unreachable or hardly reachable. In this application, two cases have to be considered. First, the two-wheeled vehicle is not guaranteed to keep moving all the time and

The current issue and full text archive of this journal is available at **www.emeraldinsight.com/0143-991X.htm**

Industrial Robot: An International Journal
38/1 (2010) 76–85

[DOI 10.1108/01439911111097878]

The authors gratefully acknowledge Yingjie Sun for his contributions to the revision of this paper.

Industrial Robot: An International Journal
Volume 38 · Number 1 · 2010 · 76–85

may fall down when unpredictable collision or other disturbances occur. Second, the initial swing-up of the vehicle with its body lying on the ground beforehand should be settled. In both cases, the ability to perform self-tilt-up motion is necessary.

Little work has been carried out to implement self-tilt-up motion for two-wheeled inverted pendulum. Samuel *et al.* (2001) presented the tilt-up motion of a single-wheel robot (called Gyrover). The spinning flywheel in Gyrover acts as a gyroscope to stabilize the robot and it can be tilted to achieve steering. They claimed that the robot is able to recover from falling by tilting the flywheel according to the conservation of angular momentum. The mechanism detail of the tilt-up motion for the single-wheel robot is described. Seong and Takahashi (2007) developed a wheeled inverted pendulum-type assistant robot called I-PENTAR, a robot that has three types of motions: inverted mobile, standing and sitting. Here, the standing motion differs from the self-tilt-up motion. In former standing motion, the body of I-PENTAR does not lie on the ground completely. The body still stands erect during standing and sitting movement. This is different from our self-tilt-up motion.

In this paper, we apply precessional motion to self-tilt-up motion. Precessional motion is a fixed-point rigid motion with a rigid body high spinning. We settle a flywheel in the body of vehicle as a rigid body. As shown in Figure 1, the flywheel is settled inside the body and a top motor drives the flywheel to spin. In order to get high-speed spinning, the reduction gearbox of top motor is removed. The simplified configuration of vehicle is shown in Figure 2. How the vehicle operates to realize self-tilt-up motion will be presented in Section 2.

The rest of the paper is organized as follows. Section 2 gives an overview of the modeling and the dynamic analysis. The mechanism of self-tilt-up motion of this model is demonstrated. Section 3 contains both simulation and experimental results. To get the simulation results, we make use of the most widely used mechanical system simulation software MSC.ADAMS. To verify the simulation results, we perform experiments with a two-wheeled inverted pendulum prototype (shown in Figure 3) and present the results. In Section 4, we conclude this paper and discuss the future work.

2. Modeling and analysis

2.1 Mechanism

To perform self-tilt-up motion, two problems should be addressed: resistance generated by gravity of body and forces that drive the body to tilt up.

Figure 1 3D model

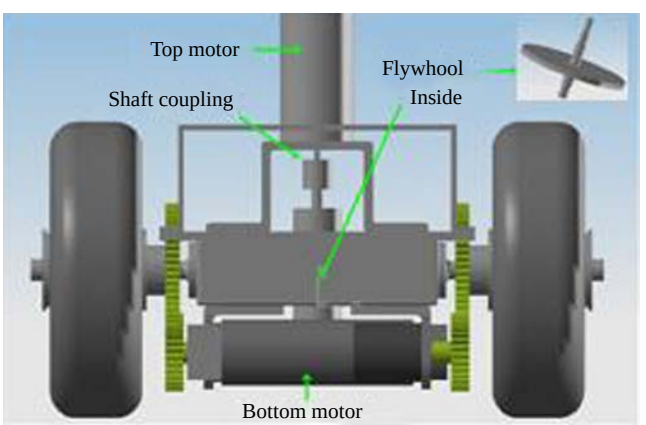

Figure 2 Simplified configuration

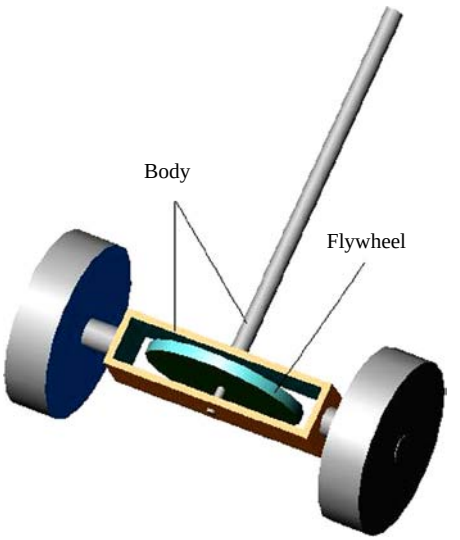

Figure 3 Prototype

2.1.1 Gravitational resistance

In precessional motion (Figure 4), it is the gravitational moment that causes the high-speed spinning body (like spinning top) to make precession around a fixed point. When the body does not spin, the gravity leads it to fall down. The gravity acts differently if the body spins at different speeds. Enlightened by this phenomenon, we settle a symmetrical part, a flywheel (shown in Figure 1), inside the two-wheeled inverted pendulum. The gravity of the body of inverted pendulum will cause the body to exhibit precession just like the spinning top when the flywheel spins at high speed. To apply this approach, first we need to find a point in the body that is fixed during the movement. Naturally, the midpoint of axis O between the two wheels is chosen to be the fixed point. To ensure that this point is fixed, we perform the force analysis (shown in Figure 5).

Figure 4 Precessional motion

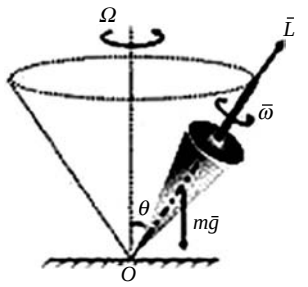

Figure 5 Coordinate system

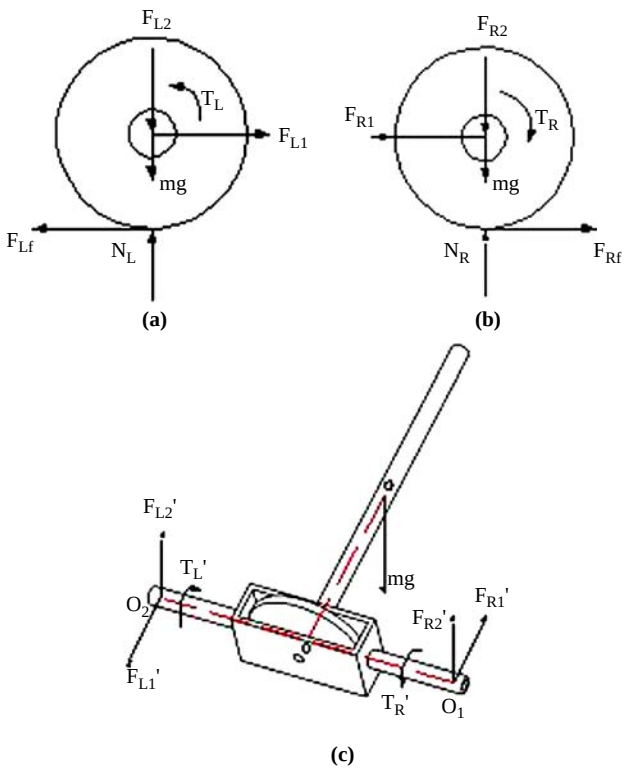

Notes: (a) Left wheel; (b) right wheel; (c) body and flywheel

For the left wheel and the right wheel, we have:

$$\begin{cases} F_{L2} + m_w g = N_L \\ F_{Lf} - F_{L1} = m_w a_L \\ T_L - F_{Lf} R = I_w \varepsilon_L \\ F_{Lf} = \mu N_L \\ a_L = \varepsilon_L R \end{cases} \quad (1)$$

$$\begin{cases} F_{R2} + m_w g = N_R \\ F_{Rf} - F_{R1} = m_w a_R \\ T_R - F_{Rf} R = I_w \varepsilon_R \\ F_{Rf} = \mu N_R \\ a_R = \varepsilon_R R \end{cases} \quad (2)$$

Here, the subscript letters L and R denote parameters of the left and right wheel, respectively. The variables in equations (1) and (2) are defined as follows:

R radius of the wheel;
I moment of inertia of the wheel;
ε angular acceleration;
a acceleration;
m_w mass of the wheel;
μ dynamic coulomb coefficient;
T torque on the wheel;
F_f friction force; and
F, N forces on the wheel.

Derived from equations (1) and (2):

$$(F_{R1} - F_{L1}) = \frac{1}{R}((T_R - T_L) - (m_w R^2 + I_w)(\varepsilon_R - \varepsilon_L)) \quad (3)$$

As it can be seen from equation (3), to guarantee the point O fixed during the movement, the force F_{R1} (F'_{R1}) should be equal to F_{L1} (F'_{L1}) and V_{o1} equal to V_{o2} (i.e. ε_R should be equal to ε_L). Thus, T_R is equal to T_L (their directions are opposite). However, it is difficult to satisfy the condition $T_R = T_L$ and $F_{R1} = F_{L1}$; we usually take the velocities V_{o1} equal to V_{o2} to approximately realize the fixed point. We find that it does not affect the self-tilt-up motion analysis. To simplify the analysis, we assume that they are equal to each other. With the point O fixed during the movement, the gravitation of body acts as moment instead of force. And the moment will cause a high-spinning rigid body and exhibits precessional motion rather than falling down.

2.1.2 The forces to perform tilt-up movement

Next, we will address how the body is to tilt up by itself. We know that the angular momentum vector $\boldsymbol{L}$ always overlaps with symmetry axis of body. Thus, the movement of vector $\boldsymbol{L}$ can represent body. According to equation $\mathbf{M} = d\mathbf{L}/dt$, the direction of the moment must point upward. Here, we assume that the wheels roll on the ground without slipping.

For system of forces on body and flywheel (treated as a whole here) in plane XOY (shown in Figures 5 and 6) about point O:

$$\begin{cases} M'_1 = -mgh\sin\theta + T'_R - T'_L = -mgh\sin\theta \\ M'_2 = (F'_{L1} + F'_{R1})d \\ M'_3 = (F'_{R2} - F'_{L2})d = 0 \end{cases} \quad (4)$$

and:

Figure 6 System of forces analysis

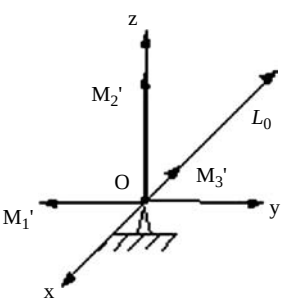

$$\begin{cases} \mathbf{M}' = M'_3 \cdot \mathbf{i} + M'_1 \cdot \mathbf{j} + M'_2 \cdot \mathbf{k} = d\boldsymbol{L}/dt \\ d\boldsymbol{L} = dL'_x \cdot \mathbf{i} + dL'_y \cdot \mathbf{j} + dL'_z \cdot \mathbf{k} \end{cases} \quad (5)$$

Here, $\mathbf{M}'$ is the external resultant moment functioning on body and flywheel.

So:

$$\begin{cases} dL'_x = 0 \\ dL'_y = M'_1 dt = -mgh \sin\theta \cdot dt \\ dL'_z = M'_2 dt = (F'_{L1} + F'_{R1})d \cdot dt \\ \mathbf{L} = \int dL'_y \cdot \mathbf{j} + \int dL'_z \cdot \mathbf{k} + \mathbf{L}_0 \end{cases} \quad (6)$$

The above component moments and component angular momentums are shown in Figures 6 and 7.

In Figure 7, moment $\boldsymbol{M}'_1$ (generated by gravity) leads initial angular momentum $\boldsymbol{L}_0$ to make precessional motion. Since $\boldsymbol{M}'_1$ is always normal to the angular momentum, $\boldsymbol{L}$, $\boldsymbol{M}'_1$ only changes the direction of $\boldsymbol{L}$. However, moment $\boldsymbol{M}'_2$ is different from $\boldsymbol{M}'_1$. The former alters the angular momentum $\boldsymbol{L}$ both in direction in and magnitude. So only moment $\boldsymbol{M}'_2$ can drive the body to tilt up. In fact, these two moments do not interfere with each other. According to instant movement analysis in Figure 7, the trajectory of body is shown in Figure 8. Rising and vibrating of body coexist, where vibrating is the result of moment $\boldsymbol{M}'_1$ and rising is due to moment $\boldsymbol{M}'_2$. As can be seen from equations (4)-(6), whether $T_R = T_L$ or $F_{R1} = F_{L1}$ does not affect the moments analysis.

Figure 7 Analysis for instant movement of body

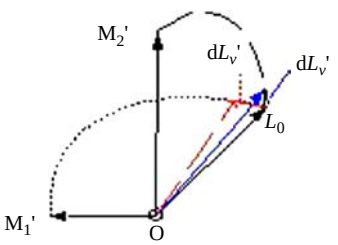

Figure 8 Trajectory of CM

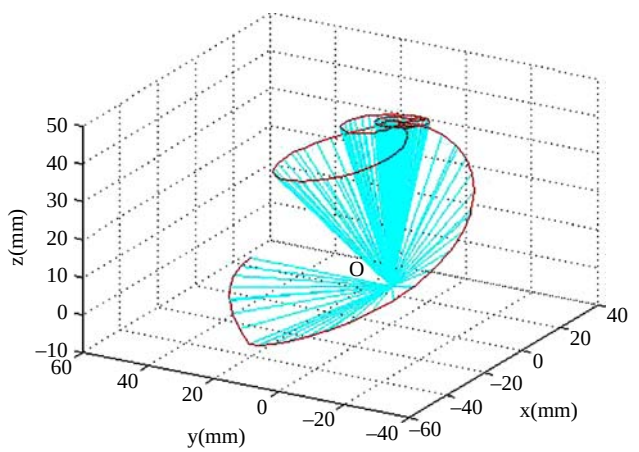

Notes: Red line is the trajectory of CM; the bottom is the point O

Since the moment $\boldsymbol{M}'_2$ tilts the angular momentum $\boldsymbol{L}$ up, to tilt up the body successfully, the moment should be large enough (the larger $\boldsymbol{L}$ will bring larger dL_z and shorter process to erect). For a prototype, its weight, height, moment of inertia, center of mass (CM), etc. are determinate. So it will realize self-tilt-up when the angular velocity of flywheel is large enough to get enough angular momentum $\boldsymbol{L}_0$ and moment $\boldsymbol{M}'_2$. In fact, with large enough $\boldsymbol{L}_0$ and $\boldsymbol{M}'_2$, the last segment of the trajectory of CM in Figure 8 gradually converges to a constant height. We prove it by both simulation (shown in Figure 13) and experiment on our prototype (shown in Figure 14).

2.2 Analysis

The two wheels have to rotate in opposite directions in order to achieve fixed-point movement. With the flywheel spinning, there exist four combinations of two-wheel rotation and flywheel spinning (shown in Figure 9).

With the moment $\boldsymbol{M}'_2$ pointing upward and the angular momentum $\boldsymbol{L}$ representing movement of body, only case (d) satisfies the condition to tilt the body up.

The above is just qualitative analysis, and we will also analyze what factors play important roles in the self-tilt-up motion. Before the derivation, we first define the notations. The body parameters have the subscript b, the flywheel parameters have the subscript r, and the wheel parameters have the subscript w. Some other definitions are listed in Table I.

The relationships of these three frames (Figures 10 and 11) are defined as follows:

1 Axis OX′ overlaps with axis OZ, axis OZ′ overlaps with negative axis OX, and axis OY′ overlaps with OY.
2 Axis OX″ overlaps with axis OX′, axis OZ″ overlaps with axis OZ′, and axis OY″ overlaps with OY′.

For the body:

$$I_1\dot{\omega}_{bx'} - (I_2 - I)\omega_{by'}\omega_{bz'} = M_{bx'} \quad (7)$$

$$I_2\dot{\omega}_{by'} - (I_3 - I)\omega_{bz'}\omega_{bx'} = M_{by'} \quad (8)$$

$$I_3\dot{\omega}_{bz'} - (I_1 - I)\omega_{bx'}\omega_{by'} = M_{bz'} \quad (9)$$

Here, the moment $M_b = [M_{bx}\ M_{by}\ M_{bz}]^{\mathrm{T}}$ represents all the external forces applied on the body. M_{bx}, M_{by} and M_{bz} represent components of M_b on axes OX′, OY′ and OZ′, respectively:

$$\begin{aligned} \mathbf{M}_b &= d\mathbf{j}_1 \times (\mathbf{F}'_{R1} - \mathbf{F}'_{L1}) + d\mathbf{j}_1 \times (\mathbf{F}'_{R2} - \mathbf{F}'_{L2}) + \mathbf{h} \\ &\quad \times \mathbf{G} + \mathbf{M}'_r + (\mathbf{T}'_R + \mathbf{T}'_L) \\ &= d(F'_{R1} + F'_{L1})\mathbf{k} - mgh\sin\theta \cdot \mathbf{j}_1 + \mathrm{M}'_r \end{aligned} \quad (10)$$

$\boldsymbol{M}'_{\mathrm{r}}$ is the moment that the flywheel function on it, and $\boldsymbol{M}'_{\mathrm{r}} + \boldsymbol{M}_{\mathrm{r}} = 0$. Besides, it we should find out the Euler's angles $q_b = (\psi_b\ \ \theta_b\ \ \phi_b)^T$ of the body frame and it is $q_b = (\omega_1\ \ \theta.0)^T$ and derives its component on body:

$$\begin{bmatrix} \omega_{bx'} & \omega_{by'} & \omega_{bz'} \end{bmatrix}^T = \begin{bmatrix} \omega_1 \sin\theta & -\dot{\theta} & \omega_1 \cos\theta \end{bmatrix}^T \quad (11)$$

Substituting equations (10) and (11) into equation (8), we obtain:

$$-I_2\ddot{\theta} - (I_3 - I_1)\omega_1^2 \sin\theta\cos\theta = -mgh\sin\theta + \mathbf{M}'_r \cdot \mathbf{j}_1 \quad (12)$$

Figure 9 Four direction combinations (a), (b), (c) and (d)

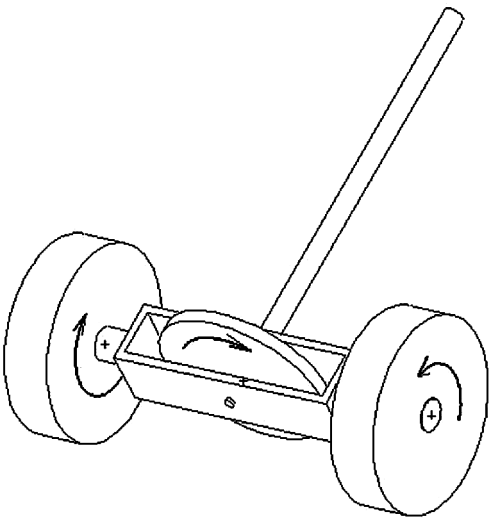

(a)

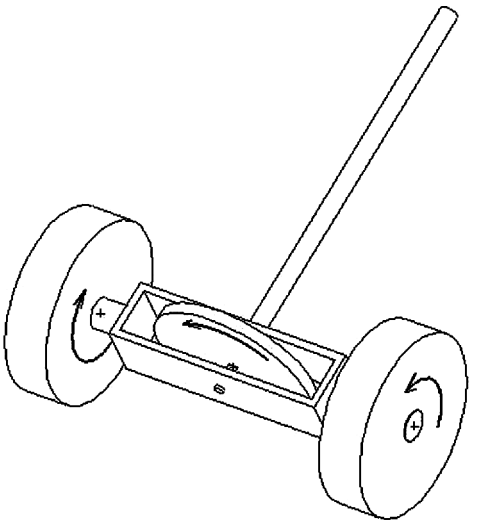

(b)

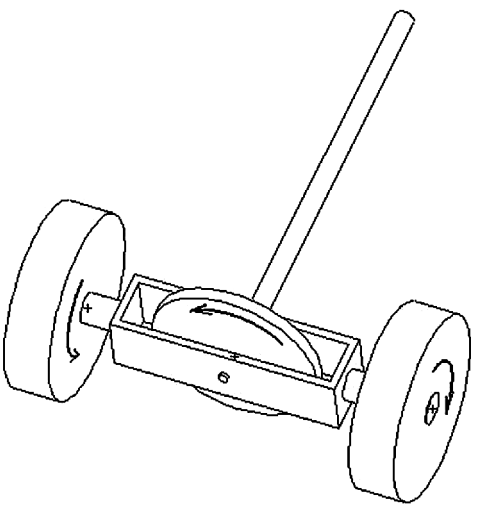

(c)

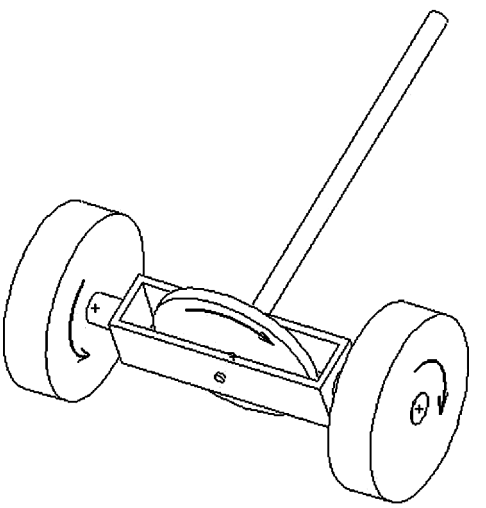

(d)

For the flywheel:

$$I'_0\dot{\omega}_{rx''} - (I'_0 - I'_1)\omega_{ry''}\omega_{rz''} = M_{rx''} \quad (13)$$

$$I'_0\dot{\omega}_{ry''} - (I'_1 - I'_0)\omega_{rz''}\omega_{rx''} = M_{ry''} \quad (14)$$

$$I'_1\dot{\omega}_{rz''} = M_{rz''} \quad (15)$$

Here, $M_r = [M_{rx}\ M_{ry}\ M_{rz}]^T$, $I_{rx'''} = I_{ry''} = I'_0$, $I_{rz''} = I'_1$. M_{rx}, M_{ry} and M_{rz} represent components of M_r on axes OX″, OY″ and OZ″, respectively.

Its Euler's angles are $q_r = (\psi_r\ \theta_r\ \phi_r)^T = (\omega_1 t + 3\pi/2\ \ \theta\ \ \pi/2 + \omega_2 t)^T$. So $\dot{q}_r = (\omega_1\ \ \dot{\theta}\ \ \omega_2)^T$ and then derives its components on flywheel:

$$\dot{\omega}_{rx''} = \omega_1 \sin\theta\cos\omega_2 t - \dot{\theta}\ sin\omega_2 t \quad (16)$$

$$\dot{\omega}_{ry''} = -\omega_1 \sin\theta\sin\omega_2 t - \dot{\theta}\ \ \sin\omega_2 t \quad (17)$$

$$\dot{\omega}_{rz''} = \omega_1\cos\theta + \omega_2 \quad (18)$$

Because the flywheel is mounted inside the body and their symmetry axes always overlap with each other, their unit vectors have the following relationship:

$$\begin{bmatrix} \mathbf{i}_1 \\ \\ \mathbf{j}_1 \end{bmatrix} = \begin{bmatrix} \cos\omega_2 t & -\sin\omega_2 t \\ \\ \sin\omega_2 t & \cos\omega_2 t \end{bmatrix} \begin{bmatrix} \mathbf{i}_2 \\ \\ \mathbf{j}_2 \end{bmatrix} \quad (19)$$

So $\mathbf{j}_1 = \sin\omega_2 t \cdot \mathbf{i}_2 + \cos\omega_2 t \cdot \mathbf{j}_2$. Substitute the relation and $\boldsymbol{M}'_{\mathrm{r}} = -\boldsymbol{M}_{\mathrm{r}}$ into equation (12) and have:

$$I_2\ddot{\theta} + (I_3 - I_1)\omega_1^2 \sin\theta\cos\theta = mgh\sin\theta + \sin\omega_2 t \cdot \mathbf{M}_r \cdot \mathbf{i}_2 + \cos\omega_2 t \cdot \mathbf{M}_r \cdot \mathbf{j}_2 \quad (20)$$

Thus, multiply $\sin\omega_2 t$ to equation (13) and $\cos\omega_2 t$ to equation (14) and substitute them into equation (20). Then, combining equations (16)-(18) and (20), we finally get:

Table I Parameters and variable name

Symbol	Parameters and variable name
O	Middle point of axis O_1O_2
d	$\|O_1O_2\| = 2d$
O − xyz	Inertial frame
$O - X'Y'Z'$, i_1, j_1, k_1	Frame attached to the body and its unit vectors
$O - X''Y''Z''$, i_2, j_2, k_2	Frame attached to the flywheel and its unit vectors
m	Mass of the body
g	gravitational acceleration
G	Gravitational center of the body
h	$h = \|OG\|$
I_1, I_2, I_3	Moment of inertia of the body
$I_{rx''}, I_{ry''}, I_{rz''}$	Moment of inertia of the flywheel
θ	Inclination angle of the body
ω_1	Angular velocity of the body about OZ axis seen from top view
ω_2	Angular velocity of the flywheel
ω_w	Angular velocity of the wheels
r	Radius of both wheels
$\omega_{bx'}, \omega_{by'}, \omega_{bz'}$	Component of absolute angular velocity of the body on frame $O - X'Y'Z'$
$\omega_{rx''}, \omega_{ry''}, \omega_{rz''}$	Component of absolute angular velocity of the flywheel on frame $O - X''Y''Z''$

Figure 10 Initial frame and body frame

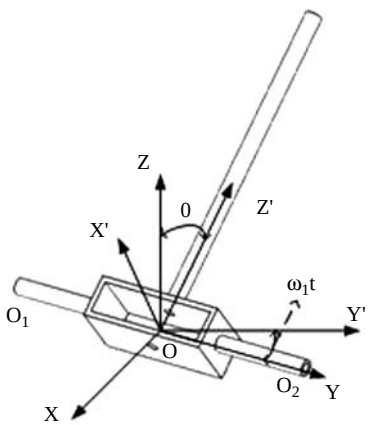

Figure 11 Flywheel frame

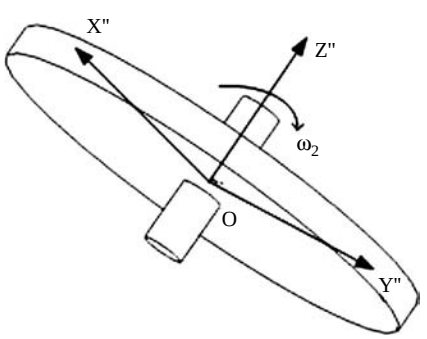

$$(I_2 + I_0')\ddot{\theta} = mgh\sin\theta - I_1'\omega_1\omega_2\sin\theta + (I_1 - I_3 + I_0' - I_1')\omega_1^2\cos\theta\sin\theta \quad (21)$$

or:

$$\ddot{\theta} = \mu(mgh - I_1'\omega_1\omega_2)\sin\theta + \lambda\omega_1^2\cos\theta\sin\theta \quad (22)$$

Here:

$$\mu = 1/(I_2 + I_0'), \quad \lambda = (I_1 - I_3 + I_0' - I_1')/(I_2 + I_0')$$

Obviously, equation (22) is a second-order nonlinear differential equation, and its solution can be expressed as an elliptic function.

Suppose that the two-wheeled inverted pendulum initially lies on the ground, i.e. the angle $\theta = \pi/2$. When the mobile inverted pendulum drives to tilt up, the angular θ becomes less and less. So to tilt up, the acceleration of θ should be negative, i.e. $\ddot{\theta} < 0$. As $\theta = \pi/2$ at first, $\cos\theta = 0$ and $\lambda\omega_1^2\cos\theta\sin\theta = 0$, the condition for a two-wheeled inverted pendulum to tilt up is:

$$mgh - I_1'\omega_1\omega_2 < 0 \quad (23)$$

In addition, $\omega_w r = \omega_1 d$, $\omega_1 = \omega_w r/d$ so:

$$\omega_w\omega_2 > \frac{mghd}{I_1'r} \quad (24)$$

For a developed prototype, the geometric parameters like m, h, d, r and I_1' are determinate, so it is possible to realize self-tilt-up when the angular velocity of flywheel ω_2 and angular velocity of wheels ω_w are high enough to satisfy the inequality in equation (24).

2.2.1 Discussion

- Referring to inequality (24), we find that a mobile-inverted pendulum with narrow body and large wheels will be easier to perform self-tilt-up motion.
- For the purpose to self-tilt up successfully, the angular velocities ω_2 and ω_w need to be large enough to satisfy the inequality (24). But in fact, with body erecting the expression $\lambda\omega_1^2\cos\theta\sin\theta$ in equation (22) will first increase to the maximum when $\theta = \pi/4$ and then decrease to zero at $\theta = \pi/2$. Whether it is positive is a factor that holds back the self-tilt-up motion.
- For the energy concerns, the self-tilt-up process should be as short as possible. It means that the angular acceleration $\ddot{\theta}$ should be large enough. So choosing ω_2 and ω_w just to meet the condition in inequality (24) is not enough. The self-tilt-up motion should be completed in several seconds to save energy.
- With flywheel angular velocity ω_2 determinate, how will the $\ddot{\theta}$ change when ω_1 increases? As it can be seen from equation (22), let ω_1 change to $\omega_1 + \Delta\omega_1$ and:

$$\begin{aligned}\delta &= \ddot{\theta}(\omega_1 + \Delta\omega_1) - \ddot{\theta}(\omega_1) \\ &= -\mu I_1'\omega_2\Delta\omega_1\sin\theta + 2\lambda\omega_1\Delta\omega_1\cos\theta\sin\theta \\ &= -\mu\Delta\omega_1\sin\theta(I_1'\omega_2 - 2(I_1 - I_3 + I_0' - I_1')\omega_1\cos\theta)\end{aligned} \quad (25)$$

where regarding $\ddot{\theta}$ as the function of ω_1 and neglecting the second-order part of $\Delta\omega_1$. In our prototype, we have:

$I_1'\omega_2 - 2(I_1 - I_3 + I_0' - I_1')\omega_1\cos\theta > 0$. Therefore, $\delta < 0$.

Thus, with ω_1 increasing (need ω_w increasing), the magnitude of the angular acceleration $\ddot{\theta}$ will increase too. So the faster the wheels rotate, the shorter the process of self-tilt-up motion will be. However, when the wheels rotate faster, it means much more energy is consumed (For the moment inertia of body is much larger than that of flywheel.) So there exists an optimal velocity to minimize the energy consumption. For different prototype, the proper angular velocity of wheels is different, which is also relative to the angular velocity of flywheel. Usually, the optimal parameters are determined by experiments.

- When the pendulum body first tilts up to top, the angular velocity relative to axis O_1O_2 is not zero. So it will fall down at the top position and then repeat the tilt-up motion until the angular velocity becomes zero at last. Thus, the self-tilt-up motion is a multiply periodic process, which will be illustrated in Section 3.
- As shown in equation (22), if the angular velocities ω_1 and ω_2 are determined, the inclination angle of the body $\boldsymbol{\theta}$ is a function of time t. Generally, it is helpful to know the numerical value of t when $\boldsymbol{\theta} = 0$. As mentioned before, the solution for equation (22) can be expressed as an elliptic function. The solution of (22) is:

$$t = \frac{1}{\sqrt{2\eta}} F(\theta) \tag{26}$$

where:

$$F(\theta) = \int_{\theta}^{\pi/2} \frac{1}{\sqrt{\cos\beta - k^2\cos^2\beta}}\, d\beta$$

$$\eta = (I_1'\omega_1\omega_2 - mgh)/(I_2 + I_0')$$

$$k^2 = \frac{\chi}{2\eta}, \chi = (I_1 - I_3 + I_0' - I_1')\omega_1^2/(I_2 + I_0')$$

When $\boldsymbol{\theta} = 0$ (namely tilting up to upright position), F(0) is a complete elliptic integral and its value can be determined by looking up the elliptic integral table. Here, t is the first time to tilt up to vertical position because the upper limit of integration is $\pi/2$. We can also calculate other period times except the first period where the upper limit of integration is not $\pi/2$.

2.2.2 Self-tilt-up motion applied to balancing movement

For a normal mobile-inverted pendulum, the balancing of the system is only achieved by considering dynamic effects. The two wheels generally rotate in same directions. In this paper, the self-tilt-up motion is a fixed-point movement and these two wheels should rotate in opposite directions. There is a contradiction between them. We settle it by linking them in the process of movement or divide the two-wheeled inverted pendulum movement into two phases:

1 When the inverted pendulum needs start to erect with its body initially lying on the ground or falling to the ground, the vehicle is switched to perform self-tilt-up motion.
2 *Stabilizing control phase*. These two phases will switch according to the state of the system as shown in Figure 12.

3. Simulations and experiments

3.1 Simulations

According to the analysis above, a 3D model (shown in Figure 13(a)) is built in ADAMS dynamic simulation environment. In the 3D model, the dimensions of body and flywheel are shown in Figure 13(b) and (c), respectively. The diameters of both wheels are 160 mm. During the process of simulation, two wheels rotate at same speed of 500 d*time (d*time is the speed unit in ADAMS and 1d*time = 1 degree/s) in opposite directions and the flywheel spins with speed 36,000 d*time (i.e. 6,000 rpm). The height of the CM is 43.065 mm. With the ADAMS simulation, we find that trajectory of CM shows a conical helix (Figure 8). The CM height relative to time is shown in Figure 13(d). The curve in Figure 13(d) represents CM of body finally tilted up to upright position, namely the vehicle self-tilts up successfully.

3.2 Experiment

To verify the simulation results, we drive our prototype with flywheel spinning at speed about 6,000 rpm. Since the CM of prototype is difficult to measure, we use its top point instead of CM to examine if the vehicle can self-tilt up successfully. Obviously, the trajectory of top point is a three-dimensional curve. So to measure the height, a setup with three degree of freedom is built. In our experiment, there is a small omni-directional vehicle with a rod on it. (This small vehicle is placed on a piece of glass to reduce disturbance to movement of prototype.) The rod has a scale and a slide block can slide on it. Apparently, this slide block has three degree of freedoms. A second rod is mounted with one end attached to the slide block. Another end of the latter rod links with a hinge joint to the top of the body. The second rod is level placed horizontally. Therefore, the scale of slide block is just the height of top point of body during the self-tilt-up movement. We record some scales of slide block and fit them as a curve. This curve is shown in Figure 14(b).

The height of the prototype is 480 mm. The diameters of both wheels are 160 mm and weight of body is about 3.2 kg. The distance between centers of two wheels is 300 mm. As shown in Figure 14(a), the height of box of body is 180 mm and the CM of body is about 198 mm. The moment of inertia of flywheel about its axis of rotation is $3.9997 \times 10^{-4}\,\mathrm{kgm}^2$. (The flywheel here is different from that in ADAMS environment.) As shown in Figure 1, there are two gears at each side. The teeth number in the gears are 40 and 70, respectively; therefore, the drive ratio is $i = 70/40 = 1.75$. The measured rotational velocity of output axis of gear box is about $88.4\,\mathrm{s}^{-1}$. Applying the above parameters to inequality (24) and the result is shown in Figure 14(b). In fact, according to inequality (24):

$$\omega_w = 88.4/i = 50.51\,\mathrm{s}^{-1},$$

$$\omega_2 = 6,000\,\mathrm{rpm} = 6,000 \times 2 \times 3.1416/60$$

$$= 628.319\,\mathrm{s}^{-1}\mathrm{m} = 3.2\,\mathrm{kg},$$

$$g = 9.8\,\mathrm{m/s}^2, h = 0.198\,\mathrm{m},$$

$$d = 0.15\,\mathrm{m}, I_1' = 3.9997 \times 10^{-4}\,\mathrm{kgm}^2, r = 0.08\,\mathrm{m},$$

$$\omega_w\omega_2 = 3.174 \times 10^4 \mathrm{mghd}/I_1' r = 2.911 \times 10^4$$

The calculation result is consistent with inequality (24). The simulation model in Section 3.1 does not equate

Figure 12 Switching between two phases

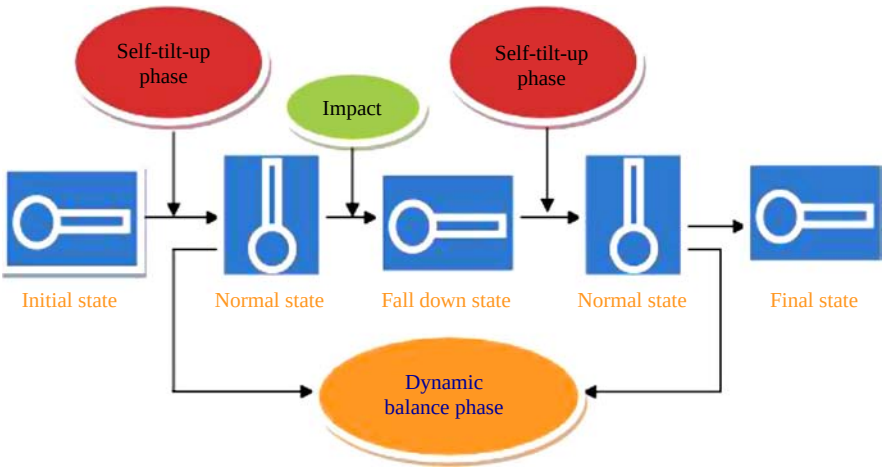

prototype in Section 3.2 because some parameter of prototype is hard to measure. In fact, the configuration of 3D model is not necessary to be exactly the same as the prototype. As it can be seen from Figures 13(b) and 14(b), these two curves are similar. Thus, we can conclude that the above analytic methods are valid and the derived results are creditable.

In addition, as the solution for equation (22) is just result of a period, to demonstrate how the angular velocity of flywheel ω_2 and wheels speed ω_w affect the self-tilt-up motion, we adopt the simulation method to verify the analysis results in Section 2.2.1 discussion (d) above. Four cases simulation of this 3D model perform:

1 $\omega_2 = 6{,}000$ rpm, $\omega_w = 83.33$ rpm;
2 $\omega_2 = 6{,}000$ rpm, $\omega_w = 50$ rpm;
3 $\omega_2 = 7{,}000$ rpm, $\omega_w = 83.33$ rpm; and
4 $\omega_2 = 7{,}000$ rpm; $\omega_w = 50$ rpm.

The final results are shown in Figure 15. In this figure, it shows:

- the larger wheel angular velocity ω_w (corresponding ω_1 larger), the shorter time for the vehicle to tilt up; and
- with larger wheel angular velocity ω_w, the amplitude of vibration will decrease faster. It is convenient to move steadily.

So, we can conclude that the angular velocity of wheel plays an important role in self-tilt-up motion after the self-tilt-up motion condition in inequality (24) is satisfied.

In addition, we must consider when the switching between self-tilt-up motion and normal dynamic movement occurs. Some researchers adopt the linearized form of partial feedback in dynamic movement analysis Baloh and Parent (2003). When angle $\theta \leq 10^0$, the moment of inertia about OZ-axis can be treated as constant and the error induced by linearization is neglectable. So we define the switching time $t_{s,}$, i.e. when all the residual inclination angle $\theta \leq 10^0$. In Figure 15, the switching time are: $t_s = 3.10$ s, $t_s = 7.86$ s, $t_s = 2.84$ s and $t_s = 6.82$ s. Apparently, t_s is a function of ω_w and ω_2. With the switching time known, we can determine when the self-tilt-up motion finish and switch to dynamic balance movement. In fact, we can design a controller for the vehicle that can switch to dynamic balance movement from tilt-up motion when it first tilts up to $\theta \leq 10^0$ in the first period.

In many literatures (Ha and Yuta, 1996; Grasser *et al.*, 2002; Kim *et al.*, 2005; Jung and Kim, 2008; Ren *et al.*, 2008; Nawawi *et al.*, 2007) the prototypes have common feature: they are designed with high bodies. The vehicles are easier to control when their bodies are higher. However, for the self-tilt-up movement, higher body means more energy will be consumed. Sometimes, two-wheeled vehicle with higher body may not realize self-tilt-up movement according to inequality (24). So the layout of vehicle with self-tilt-up ability is different from the ones in the above literatures. To perform stabilizing control, the body of vehicle should be as high as possible. However, to implement self-tilt-up movement, the body of vehicle should be as low as possible according to inequality (24). Thus, a setup that can change the height of the body is necessary when the vehicle is designed to apply to environment where high body is necessary. This will be considered in our future work.

4. Conclusions

In summary, this paper presents a self-tilt-up motion for a two-wheeled inverted pendulum. With the analysis of the dynamics, simulation demonstrations and prototype development, the results show that the vehicle could perform self-tilt-up motion without any assistance. The principle of this self-tilt-up motion involves processional motion of rigid body. We also pointed out the factors that play important roles in influencing the performance of self-tilt-up motion and then define the switching time for the motion to switch to dynamic balance movement. As a future work, we will design a controller that can drive the vehicle to perform self-tilt-up motion and dynamic balance movement smoothly.

Traditional multi-wheels robots cannot work when they overturn. However, the two-wheeled inverted pendulums with self-tilt-up ability do not have this shortcoming. They can stand up to keep working even if they fall down. A two-wheeled inverted pendulum with self-tilt-up ability can be applied to many places. Equipped with solar battery, it can be used as an independent explorer. We can also deploy this type of vehicle in swarms for planetary detection. For example, many small two-wheeled inverted pendulums assist a lunar rover for exploration, samples gathering, etc. Interesting directions for future work include the cooperation of the two-wheeled inverted pendulums.

Figure 13 CM height of 3D model

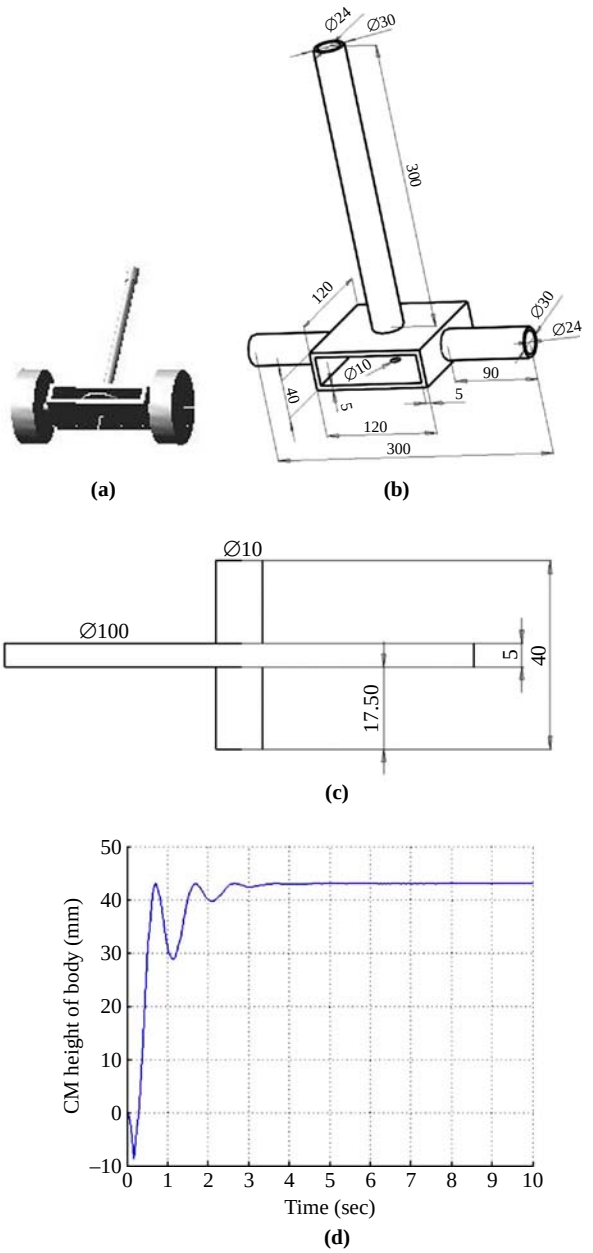

Notes: (a) The simplified 3D model; (b) dimensions of body; (c) dimensions of flywheel; (d) CM height of body

Figure 14 Top point height of prototype

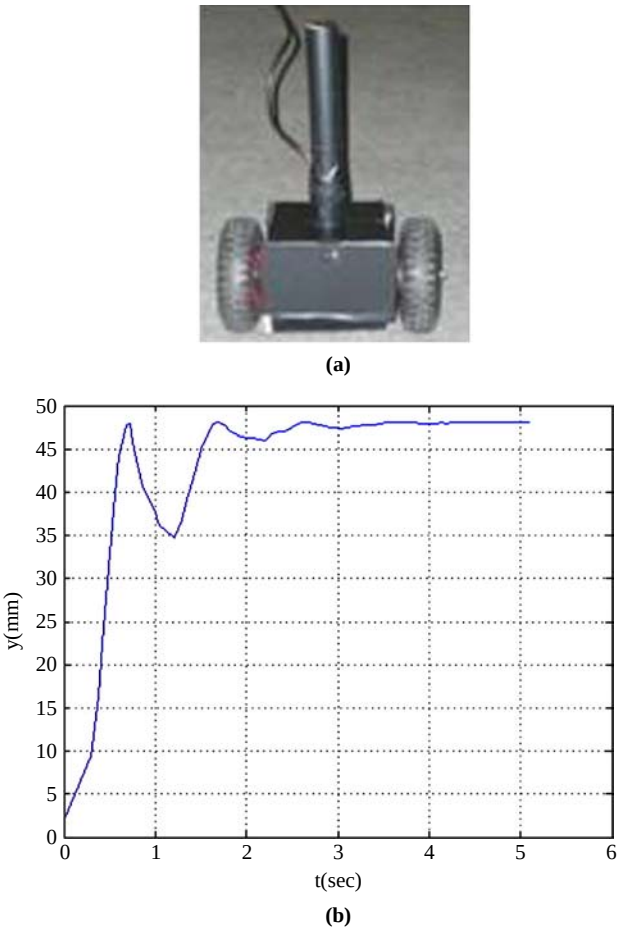

Notes: (a) Prototype; (b) top point height with flywheel spinning

Figure 15 Simulation results

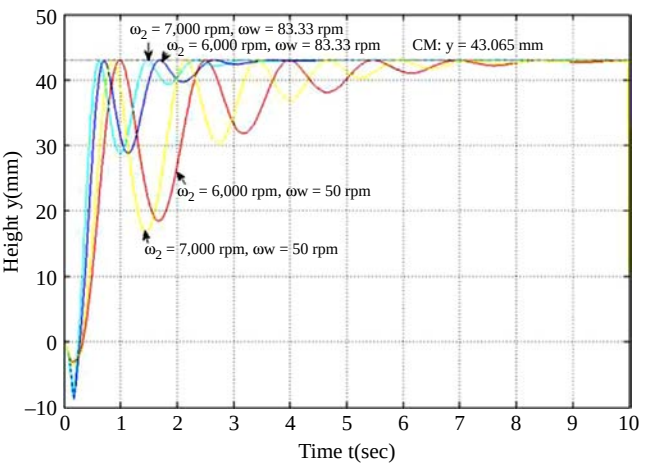

References

Baloh, M. and Parent, M. (2003), "Modeling and model verification of an intelligent self-balancing two-wheeled vehicle for an autonomous urban transportation system", in Michael, B. and Michael, P. (Eds), paper presented at the Conference on Computational Intelligence, Robotics, and Autonomous Systems, Singapore, December 15.

Grasser, F., D'Arrigo, A., Colombi, S. and Rufer, A. (2002), "JOE: a mobile, inverted pendulum", *IEEE Transactions Industrial Electronics*, Vol. 49 No. 1, p. 107.

Ha, Y.-S. and Yuta, S. (1996), "Trajectory tracking control for navigation of the inverse pendulum type self-contained mobile robot", *Robotics and Autonomous Systems*, Vol. 17 Nos 1-2, pp. 65-80.

Jung, S. and Kim, S.S. (2008), "Control experiment of a wheel-driven mobile inverted pendulum using neural network", *IEEE Transactions on Control Systems Technology*, Vol. 16 No. 2, pp. 297-303.

Kim, Y., Kim, S.H. and Kwak, Y.K. (2005), "Dynamic analysis of a nonholonomic two-wheeled inverter pendulum robot", *Journal of Intelligent and Robotic Systems: Theory and Applications*, Vol. 44 No. 1, pp. 25-46.

Nawawi, S.W., Ahmad, M.N. and Osman, J.H.S. (2007), "Development of a two-wheeled inverted pendulum mobile robot: research and development, SCOReD 2007", 5th Student Conference on 12-11 December, pp. 1-5.

Pathak, H., Jaume, F. and Sunil, K.A. (2005), "Velocity and position control of a wheeled inverted pendulum by partial feedback linearization", *IEEE Transaction on Robotics*, Vol. 21 No. 3, pp. 505-13.

Ren, T.-J., Chen, T.-C. and Chen, C.-J. (2008), "Motion control for a two-wheeled vehicle using a self-tuning PID controller", *Control Engineering Practice*, Vol. 16 No. 3, pp. 365-75.

Samuel, K.W., Au, Y.X. and Wilson, W.K.Y. (2001), "Control of tilt-up motion of single wheel robot via model-based and human-based controllers", *Mechatronics*, Vol. 11 No. 4, pp. 451-73.

Segway Human Transporter (2004), available at: www.segway.com

Seong, H.J. and Takahashi, T. (2007), "Wheeled inverted pendulum type assistant robot: inverted mobile, standing, and sitting motions", paper presented at IROS 2007: IEEE/RSJ International Conference on Intelligent Robots and Systems, October 29-November 2, San Diego, CA, USA, pp. 1932-7.

Corresponding author

Shouhong Miao can be contacted at: motsler@sjtu.org